Cell, Vol. 100, 447–456, February 18, 2000, Copyright ©2000 by Cell Press

Crystal Structure of the VHS and FYVE Tandem Domains of Hrs, a Protein Involved in Membrane Trafficking and Signal Transduction

Yuxin Mao,* Alexei Nickitenko,† Xiaoqun Duan,‡ Thomas E. Lloyd,§ Mark N. Wu,§ Hugo Bellen,‡§‖ and Florante A. Quiocho*†‡#

*Structural and Computational Biology and Molecular Biophysics Graduate Program
†Department of Biochemistry and Molecular Biology
‡Howard Hughes Medical Institute
§Department of Molecular and Cellular Biology
‖Department of Molecular and Human Genetics
Baylor College of Medicine
Houston, Texas 77030

Summary

We have determined the 2 Å X-ray structure of the 219-residue N-terminal VHS and FYVE tandem domain unit of *Drosophila* Hrs. The unit assumes a pyramidal structure in which the much larger VHS domain (residues 1–153) forms a rectangular base and the FYVE domain occupies the apical end. The VHS domain is comprised of an unusual "superhelix" of eight α helices, and the FYVE domain is mainly built of loops, two double-stranded antiparallel sheets, and a helix stabilized by two tetrahedrally coordinated zinc atoms. The two-domain structure forms an exact 2-fold-related homodimer through antiparallel association of mainly FYVE domains. Dimerization creates two identical pockets designed for binding ligands with multiple negative charges such as citrate or phosphatidylinositol 3-phosphate.

Introduction

Intracellular membrane trafficking events are tightly regulated to ensure proper spatial and temporal delivery of vesicular cargo. One excellent example of this regulation is the ligand-dependent endocytosis of growth factor receptors. After ligand binding and receptor activation, a series of phosphorylation events leads to the recruitment of clathrin at the site of the activated receptor complex. The plasma membrane containing the receptor pinches off from the membrane to form a clathrin-coated vesicle, the clathrin cage is actively disassembled, and endocytic vesicles fuse with one another to form early endosomes. Next, endosomal cargo is sorted either to recycling endosomes, where it is returned to the plasma membrane, or to the lysosome, where it is degraded. In this way, signal transduction pathways can be regulated by controlling the level of activated receptor present on the surface of the cell. Little is known about how the balance between surface recycling and lysosomal degradation of endosomal cargo is achieved. Some endosomal proteins such as tyrosine kinase receptors are primarily trafficked to lysosomes whereas others such as the transferrin receptor are recycled back to the plasma membrane. Regulatory molecules that mediate this trafficking decision might be expected to interact with cargo proteins, membrane phospholipids, and members of the trafficking machinery.

One potential candidate that satisfies these criteria is a newly identified protein named Hrs (hepatocyte growth factor regulated tyrosine kinase substrate). As its name implies, Hrs is tyrosine phosphorylated in response to a variety of growth factors including HGF, EGF, and PDGF (Komada and Kitamura, 1995). Hrs is expressed in the cytoplasm of all cells and is predominantly localized to endosomes (Komada et al., 1997). This localization is consistent with the finding that Vps27p, the yeast homolog of Hrs, is also expressed on endosomes, and null mutants are unable to traffic most proteins to the vacuole (yeast equivalent of the lysosome), leading to an exaggerated "class E" compartment (Piper et al., 1995). Similarly, mice lacking Hrs die early in embryonic development and have abnormally enlarged endosomes (Komada and Soriano, 1999). Thus, Hrs has been proposed to play a role in trafficking cargo from the endosome to the lysosome. Interestingly, Hrs has also been implicated in exocytosis of synaptic vesicles. A splice variant of rat Hrs named Hrs-2 is a calcium-dependent ATPase, tightly binds the t-SNARE SNAP-25, and inhibits neurotransmitter release when injected into permeabilized PC12 cells (Bean et al., 1997). This suggests that Hrs may regulate synaptic vesicle exocytosis by directly interacting with the fusion machinery.

Hrs contains several conserved domains that are present in proteins implicated in signal transduction and/or membrane trafficking. The VHS (Vps27p, Hrs, STAM) domain is present at the amino terminus of several proteins believed to play a role in tyrosine kinase receptor signaling. STAM (signal-transducing adaptor molecule) is tyrosine phosphorylated by Jak3 and Jak2 tyrosine kinases in response to cytokines IL-2 and granulocyte-macrophage colony-stimulating factor (GM-CSF) (Takeshita et al., 1996, 1997). Interestingly, Hrs is also phosphorylated in response to these cytokines and binds to STAM via a coiled-coil domain (Asao et al., 1997). Another VHS-containing protein called EAST (epidermal growth factor receptor-associated protein with SH3 and TAM domains) is tyrosine phosphorylated by the activated EGF receptor, colocalizes with clathrin, and coimmunoprecipitates eps15, an essential component of the ligand-dependent endocytic machinery (Carbone et al., 1997; Lohi et al., 1998). Although the function of the VHS domain is not yet known, its presence in STAM, EAST, and Hrs strongly suggests a role for this domain in tyrosine kinase receptor-mediated endocytosis (Lohi and Lehto, 1998).

Another interesting domain of Hrs is the FYVE (Fab1p, YOTB, Vac1p, and EEA1) zinc finger domain present in over 40 proteins. This domain has been shown by several groups to specifically bind phosphatidylinositol 3-phosphate (PI(3)P) via a conserved (R/K)(R/K)HHCR

#To whom correspondence should be addressed (e-mail: faq@bcm.tmc.edu).

Table 1. Crystallographic Analysis Statistics

A. Data Collection

Crystal	Wavelength (Å)	d_{min} (Å)	Number of Measurements	Unique Reflections	Completeness (%)	$\langle I \rangle / \langle \sigma \rangle$	R_{sym}[a,b] (%)
MAD phasing data	SeMet λ_1 (0.9793)	2.3	109,669	29,093	99.6 (100)	20.9 (4.8)	5.8 (23.1)
	SeMet λ_2 (0.9788)	2.3	109,815	29,025	99.6 (100)	22.4 (4.9)	5.4 (22.5)
	SeMet λ_3 (0.9717)	2.3	110,340	29,555	99.7 (100)	20.0 (4.3)	6.0 (25.9)
Refinement data	SeMet λ_3 (0.9717)	2.0	89,859	22,957	99.8 (100)	15.0 (3.7)	7.0 (29.1)

B. Phasing

Observed Diffraction Ratios[c]

	λ_1	λ_2	λ_3
λ_1	0.045	0.024	0.033
λ_2		0.052	0.022
λ_3			0.047

Figure of merit (FOM) 0.51

C. Refinement

Resolution Range (Å)	R_{value}[d] (%)	R_{free}[e] (%)	Bond Length Deviation (Å)	Bond Angle Deviation (°)	Bonded Main Chain Atom B Factor Rmsd (Å^2)	Bonded Side Chain Atom B Factor Rmsd (Å^2)
50-2.0	21.5	25.4	0.016	1.6	0.53	0.45

[a] Values in parentheses are for the outer resolution shell.
[b] $R_{sym} = \Sigma_h \Sigma_i |I_i(h) - \langle I(h) \rangle| / \Sigma_h \Sigma_i I_i(h)$.
[c] Values are $\langle (\Delta |F|)^2 \rangle^{1/2} / \langle |F|^2 \rangle^{1/2}$.
[d] $R_{value} = \Sigma (|F_{obs}| - k|F_{cal}|) / \Sigma |F_{obs}|$.
[e] R_{free} is obtained for a test set of reflections, consisting of a randomly selected 10% of the data and not used during refinement.

motif (Stenmark et al., 1996; Burd and Emr, 1998; Gaullier et al., 1998; Patki et al., 1998). The rab5 effector EEA-1 (early endosomal antigen 1), one of the best characterized FYVE-containing proteins, is essential for the tethering and fusion of early endosomes (Christoforidis et al., 1999). The endosomal localization of EEA-1 is disrupted by deletion of the FYVE domain or by treatment with the PI3-kinase inhibitor wortmannin, suggesting that EEA-1 binding to endosomes is mediated by the FYVE-PI(3)P interaction (Stenmark et al., 1996; Simonsen et al., 1998). In other FYVE domain–containing proteins such as Hrs and Vac1p, on the other hand, proteins deleted of the FYVE domain still localize to endosomes (Komada et al., 1997; Tall et al., 1999). Furthermore, Vac1p membrane localization is not disturbed in the *Vps34* (PI3-kinase) null mutant, suggesting that PI(3)P is not essential for Vac1p binding to membranes (Tall et al., 1999). Although wortmannin does inhibit Hrs membrane localization, the endosomal location of Hrs lacking the FYVE domain suggests that interactions with other PI(3)P-binding proteins mediate its localization (Komada and Soriano, 1999). Thus, the FYVE domain is required for membrane localization in some but not all FYVE-containing proteins, making it likely that this domain plays other roles as well.

As a first step in understanding the function of Hrs at the atomic level, we have determined the crystal structure of the N-terminal 219 amino acids of *Drosophila melanogaster* Hrs containing the VHS and FYVE domains. This report describes a prototypic structure for the VHS domain that is conserved in over 20 proteins. Moreover, although the structure of the Hrs FYVE domain is very similar to that recently reported for Vps27p (Misra and Hurley, 1999), our data suggest a significantly different model for binding of the FYVE domain to PI(3)P and membranes.

Results and Discussion

Structure Determination and Overall Structure

The tandem domain segment (residues 1 to 219) of *Drosophila* Hrs was obtained by subcloning and overexpression in a protein-splicing system and yielded excellent crystals (see the Experimental Procedures). The presence of citrate and maintaining the pH at 7.2 were crucial in obtaining the crystals. The crystals belong to the C2 space group with unit cell dimensions of a = 116.71 Å, b = 69.67 Å, c = 41.80 Å, and β = 94.77° and one molecule in the asymmetric unit. The structure was determined by selenomethionine MAD phasing (Table 1). With the exception of residues 146–148, which were assumed to be very flexible, all residues were positioned in well-defined density. The current model refined at 2 Å resolution has an R value of 21.5% and an R_{free} of 25.4%. The model has good geometry (Table 1), and 99.5% of the backbone dihedral angles are in the most favored or allowed regions.

The three-dimensional structure of the VHS and FYVE tandem domains is illustrated in Figure 1A. Both domains are aligned to form a pyramid-like structure with the much larger VHS domain forming a rectangular base (45 Å × 35 Å) with a thickness of about 1/3 of the pyramid altitude (~60 Å) and the FYVE domain occupying the apical end. Following termination of the VHS domain at Asp-153, which is salt linked to Lys-71, the polypeptide chain turns sharply into an N-terminal segment of the FYVE domain. The VHS domain has a long C-terminal segment which, together with the N-terminal segment of the FYVE domain, could serve as a flexible tether between the two domains. As will be discussed below, the tandem domain unit associates into a homodimer, and this association may provide high specificity and affinity of ligand binding.

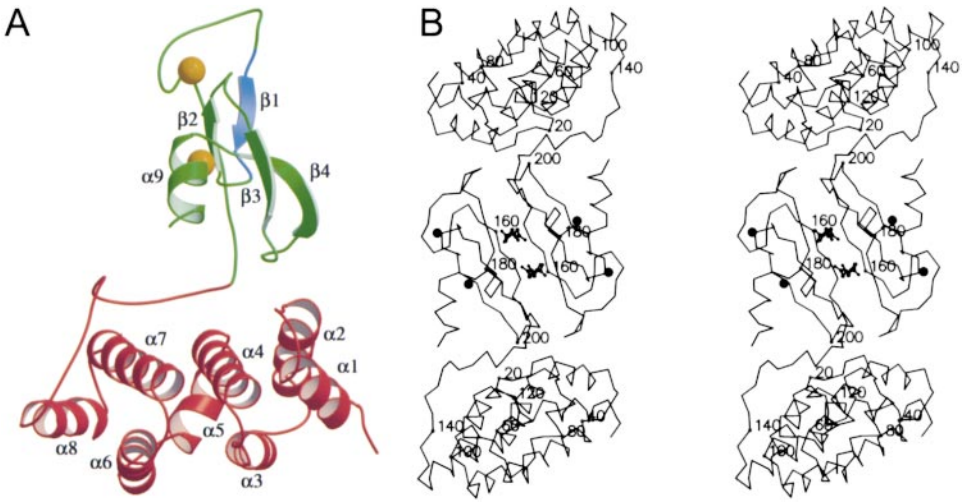

Figure 1. Structure of the Hrs Tandem Domains of VHS (Residues 1–153) and FYVE (Residues 154–219)

(A) Ribbon representation of the overall fold of the tandem domains of VHS (red) and FYVE (green) with the secondary structure labeled and bound Zn^{2+} atoms represented by gold spheres. α helices 1, 3, and 6 constitute the A helices of the three repeats of the VHS domain, whereas 2, 4, and 7 α helices make up the B helices. The segment of the FYVE domain highlighted in blue, which includes β1 strand, contains 176RKHHCR, a sequence motif conserved among FYVE domains.

(B) Stereoview of the tandem domain homodimer down the "front" or crystallographic 2-fold rotation axis. Every 20 residues are numbered and identified with small filled circles. The two large filled circles represent Zn^{2+}. Figures 1, 5A, 5C, and 6 were drawn using Molscript (Kraulis, 1991), Raster3D (Merritt and Bacon, 1997), and/or Bobscript (Esnouf, 1997).

VHS Domain: A Motif of Superhelix of Helices

The structure of the VHS domain (residues 1–153) is comprised of eight α helices and a long C-terminal extension (Figures 1A and 1B). The first four helices (α1 to α4) form two repeats, each consisting of two antiparallel helices (A and B). The succeeding three helices (α5 to α7) fold into a three-helix hairpin (repeat 3) with α6 and α7 analogous to the A and B helices, respectively, of the first two repeats. The α8 helix is packed against α6 and α7. Repeat 1 helices (α1 and α2) are related to their counterparts of repeat 2 (α3 and α4, respectively) by a left-handed rotation of ~20° about an axis roughly perpendicular to the helices. Helices α3 and α4 of repeat 2 are, in turn, stacked essentially in parallel with α6 and α7 of repeat 3. These interrepeat geometries give rise to a left-handed shallow groove, in which the A helices are located at the outer (convex) face and form the bottom of the pyramid-like structure and the B helices are located at the inner (concave) face at approximately 1/3 of the height of the pyramidal structure.

The parallel stacking of the A and B helices of the three repeats, combined with α8, creates a hydrophobic channel between the double layer of helices that nearly spans the entire length of the VHS domain. The channel contains mostly hydrophobic residues (~30), of which 80% are conserved among known VHS domains (Figure 2). The slightly wider space in the channel between the two-helix repeat 2 and the three-helix repeat 3 (Figure 1A) has the highest concentration of hydrophobic residues, mostly with aromatic and large aliphatic side-chains. The distribution pattern of hydrophobic residues in the channel is a major determinant of the packing geometry of the superhelical structure of the VHS domain.

Comparison of the VHS Domain with Other Superhelix Motifs

Superhelices of α helices have been observed previously in domains (Das et al., 1998) and subunits of a variety of enzymes and signaling proteins, one of which is clathrin, a key player in endocytosis (Raag et al., 1988; Thunnissen et al., 1994; Huber et al., 1997; Strickland et al., 1998; Groves et al., 1999; Vetter et al., 1999). The first two repeats of the VHS domain are very similar to the HEAT repeats, whereas the third repeat closely resembles an ARM repeat (Figure 3A). The combination of two different repeats makes the VHS domain an unusual member of domains or proteins with superhelical structures.

The closest geometrical match to the three repeats plus the eighth helix of the VHS domain occurs in the phosphatase 2 PR65/A subunit (Groves et al., 1999), in which the HEAT repeats 3 to 5 plus helix A of repeat 6 superimpose with an rms deviation of 3.6 Å over 128 residues (DALI [Holm and Sander, 1995]) "Z" score of 9.1) (Figure 3B). The closer match with the PR65/A subunit is attributable to the similarity of the left-handed packing geometry between repeats 1 and 2 to that between repeats 3 and 4 of the PR65/A subunit. Moreover, the VHS domain and PR65/A subunit are the only ones, thus far, that have a left-handed superhelical fold of α helices. Although the amino acid sequences of the overlapped VHS and PR65/A repeats differ considerably, the hydrophobic nature of the channels is conserved (Figure 2).

Multipurpose Docking Sites of the VHS Domain

The superhelical structure found in the phosphatase 2 PR65/A subunit and other subunits and protein domains

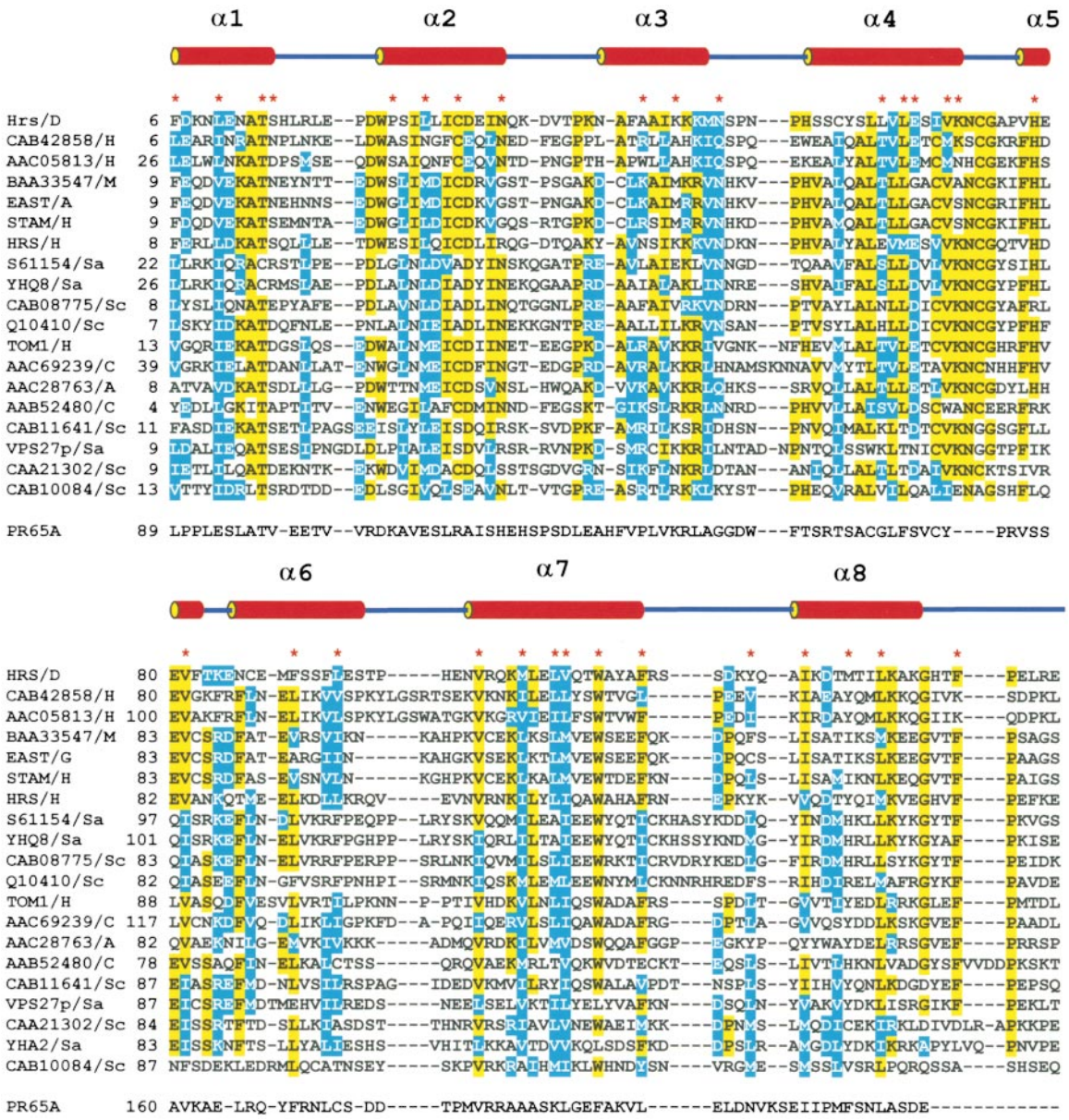

Figure 2. Multiple Sequence Alignment of VHS Domains Constructed Using the Clustal W Program and Colored by the Boxshade Program

Search of sequences similar to the *Drosophila* VHS sequence was performed using BLAST2 (Altschul et al., 1997). The alignment with the HEAT repeats 3 to 5 and the A helix of repeat 6 of the X-ray structure of the PR65/A subunit of protein phosphatase 2 is based on DALI (Holm and Sander, 1995). The α helices of the Hrs VHS structure are shown above the alignment. The first column gives the name of the protein or the accession number in the Entrez database for those proteins that have not been characterized. The following capital letters designate the species (A, *Arabidopsis thaliana*; C, *Caenorphabditis elegans*; D, *Drosophila melanogaster*; G, *Gallus gallus*; H, *Homo sapiens*; M, *Mus musculus*; Sa, *Saccharomyces cerevisiae*; and Sc, *Schizosaccharomyces pombe*). Identical and similar residues have yellow and blue backgrounds, respectively. The conserved hydrophobic residues in the VHS channel of Hrs are identified by asterisks.

serves as a scaffold for protein-protein interactions, particularly in the vicinity of the inner groove and its ridge (Raag et al., 1988; Thunnissen et al., 1994; Huber et al., 1997; Das et al., 1998; Strickland et al., 1998; Groves et al., 1999; Vetter et al., 1999). Interestingly, the VHS domain is engaged in both interdomain and dimeric interactions. The concave surface docks with the proximal end of the FYVE domain within the monomer and the apical end of the FYVE domain from the symmetry related molecule (Figures 1A and 1B). The α2 helix of the VHS domain contains three extremely conserved residues (Trp-23, Asp-31, and Leu-27) that make both intra- and intermolecular interactions with FYVE domains. Trp-23 is engaged in contacts with hydrophobic moieties at the tip of the loop between β3 and β4 strands of the FYVE domain within the monomer, whereas Asp-31 is involved in hydrogen-bonding interactions between monomers. The Oδ1 and Oδ2 of the carboxylate sidechain of Asp-31 form strong hydrogen bonds with the backbone peptide NHs of residues Phe-173 and Thr-174, respectively, at the apical loop preceeding the β1 strand of the FYVE domain from the symmetry-related

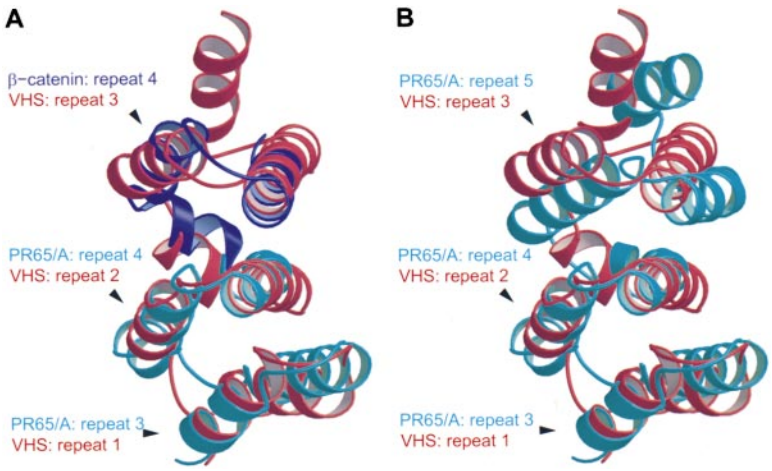

Figure 3. Overlap of the VHS Domain Helix Hairpin Repeats with Similar Repeats of Other Proteins

(A) The first two repeats of VHS (red) superimposed with HEAT repeats 3 and 4 (cyan) of protein phosphate 2 PR65/A subunit (Groves et al., 1999) and the third repeat superimposed with the ARM repeat 4 (blue) of β catenin (Huber et al., 1997).

(B) Overlap, based on DALI (Holm and Sander, 1995), of the entire eight helices of the VHS domain with repeats 3 to 5 plus the first helix of repeat 6 of protein phosphate 2 PR65/A subunit.

molecule. Furthermore, the Oδ2 also accepts a hydrogen bond from the hydroxyl sidechain of Thr-174. The third conserved VHS residue, Leu-27, is involved in hydrophobic interactions with the symmetry-related Phe-173 that is also a highly conserved residue among FYVE domains. The VHS domain is a prime example of this type of structure whose concave surface acts as a platform for both interdomain and dimeric interactions.

The VHS domain may also interact with membranes and/or proteins of the endocytotic machinery. The N-terminal portion of EAST containing the VHS domain is capable of interacting with membranes and partially colocalizes with clathrin (Lohi et al., 1998). This N-terminal VHS portion of EAST also forms a complex with eps15, an EGF receptor substrate associated with clathrin-coated pits and vesicles (Lohi and Lehto, 1998). Moreover, the presence of the VHS domain in Hrs may explain why the FYVE deletion mutant is not mislocalized (Komada et al., 1997). Thus, the VHS domain may localize proteins to the membrane through interactions with the membrane and/or the endocytic machinery. Taken together, the VHS domain is therefore viewed as a multipurpose docking adapter.

FYVE Zinc Finger Domain and Its Involvement in Dimer Formation

The structure of the FYVE domain (residues 154–219) consists of a nonstandard N-terminal strand, loops, two double-stranded antiparallel β sheets, and a C-terminal helix (Figures 1A and 1B). The fold is stabilized by a pair of bound Zn^{2+} atoms, each tetrahedrally coordinated with four Cys sidechains. The X-ray structure of the FYVE zinc finger domain of Hrs is very similar to that of the isolated monomeric FYVE domain of Vps27p (Misra and Hurley, 1999), with an rms deviation of 0.93 Å. However, our crystal structure has revealed the formation of a homodimer mainly by way of the antiparallel association between two FYVE domains (Figures 1B, 4A, and 4B). This homodimer is related by a crystallographic 2-fold axis, and this association buries a total of 1920 $Å^2$ accessible surface area. The largest area of contact between the monomers involves mainly residues from a region of the FYVE domain that includes the long N-terminal segment and the strands of the two antiparallel β sheets. An important dimeric interaction is the hydrophobic edge-on contact between two Trp-158 residues flanked by two His-179 residues (Figure 5A). This array of interactions, involving the invariant Trp-158 and His-179 residues, not only contributes to the dimer stability but also creates an environment essential to the functional role of His-179 in ligand binding (discussed further below).

Dimer formation of the FYVE domain has also been observed by other recent studies. NMR analysis demonstrated that the isolated FYVE domain of EEA1 forms functional homodimers that are in fast equilibrium with monomers (Kutateladze et al., 1999). More importantly, the analysis further indicated that the homodimers bind PI(3)P-bearing membranes much more tightly than the corresponding monomers. Binding appears to be more specific for PI(3)P since PI(5)P, a naturally occurring lipid headgroup, is bound more weakly. The suggestion that the long N-terminal segment of the EEA1 FYVE domain contributes to dimerization (Kutateladze et al., 1999) is consistent with the Hrs structure that shows the involvement of this segment in homodimer formation (see above; Figure 1B). Interestingly, the N-terminal segment of the monomeric recombinant Vps27p FYVE domain is considerably shorter as it is missing several residues (Kutateladze et al., 1999; Misra and Hurley, 1999). Using the dynamic light scattering technique, we have similarly observed a dimer-monomer equilibrium of the Hrs tandem domains in solution. Therefore, the FYVE domain of Hrs is capable of forming a homodimer. Finally, as further exemplified by the pleckstrin homology (PH) domain (Klein et al., 1998), domain oligomerization appears to be a common feature for high-affinity phosphoinositide binding.

Binding Sites in the FYVE Dimer for Ligands with Multiple Negative Charges

Our structural data have further uncovered two neighboring identical pockets formed between two symmetry-related FYVE domains (Figures 1B, 4A, and 4B). Each pocket is lined mainly by residues from the β1 strand of one FYVE domain, which contains several basic residues of the conserved 176RKHHCR motif and the β4 strand of the symmetry-related FYVE domain, which contains hydrophobic residues (Figures 1 and 5A). This pocket is ideally suited for binding ligands with multiple negative charges such as citrate (Figure 5A), an essential component in crystallization of the tandem domains. The area encompassing the two neighboring pockets

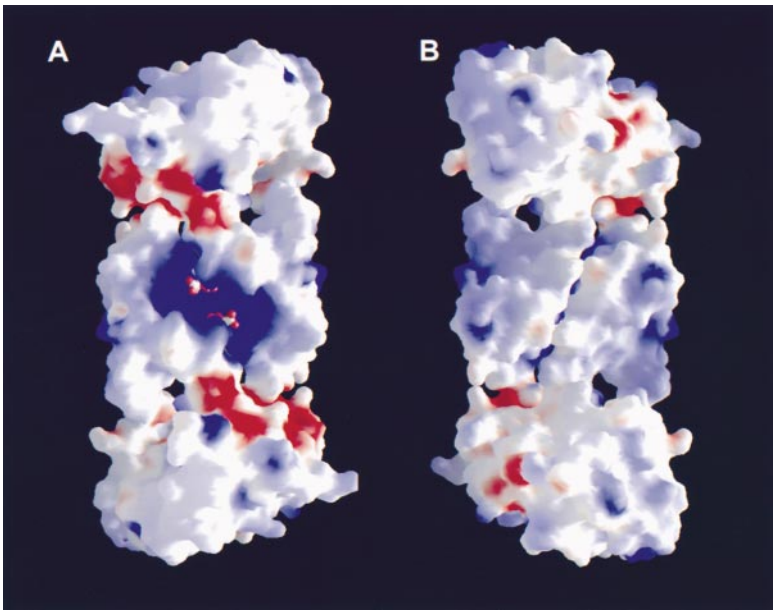

Figure 4. Electrostatic Surface Potential (±10 kT) of the Homodimer of the VHS-FYVE Tandem Domains

(A) Electrostatic surface potential was calculated and displayed within GRASP (Nicholls et al., 1993). "Front view" of the homodimer that is identical to that shown in Figure 1B. As also shown in Figure 1B, the middle of the dimer contains two symmetry-related multianion-binding pockets with bound citrates whose C1 carboxylates are partially exposed. The bound citrates are excluded from the GRASP calculation.

(B) "Back view" of the homodimer obtained by a 180° rotation of the structure shown in (A) about a vertical axis.

(named "multianion-binding sites") shows a very intense positive electrostatic surface potential (Figure 4A), largely due to the presence of two symmetry-related conserved basic sequence motifs.

Four key features are associated with molecular recognition and binding of citrate by the multianion-binding site of the FYVE dimer, and these are likely to have an important bearing on the binding of the phosphatidylinositol 3-phosphate head group. First, the citrate is bound snugly in each pocket with about 90% of its free accessible surface buried (Figure 4A). The C1 carboxylate, which is partially exposed and hydrated by three ordered surface water molecules, occupies the pocket opening, and the C5 carboxylate occupies the pocket bottom (Figures 1B, 4A, 5A, and 5B).

Second, the citrate is engaged in an extensive network of charge-coupling and hydrogen-bonding interactions mostly with the positively charged residues of the conserved motif (Figure 5B). Although Lys-177 of the motif is near the ligand-binding pocket (Figure 5A), it does not interact with the bound citrate. However, Lys-177 may stabilize the multianion-binding site by forming a salt link with Asp-160.

Third, the citrate makes a specific hydrogen bond with the invariant His-179. The hydrophobic environment of the His-179 sidechain in the pocket bottom, being flanked on both sides by Val-186 and two symmetry-related Trp-158 (Figure 5A), would seem to preclude a protonated positively charged imidazole group. As a consequence of this environment and the involvement of the His Nδ2H as a hydrogen bond donor to the peptide carbonyl oxygen of Ala-159, it is indicated that the His Nδ1 group accepts a hydrogen bond from one of the citrate carboxylates that would normally have the highest pK_a of 6.4 (Figure 5B).

Fourth, the cluster of nonpolar C2 and C4 groups of citrate interface with the nonpolar groups of Cβ and Cγ of Arg-181 and the sidechains of Ile-203, Val-207 of the b4 strand from the symmetry-related FYVE domain (Figure 5A). Ile-203 is weakly conserved, whereas Val-207 is strongly conserved among FYVE domains. As these nonpolar interactions can only occur in the dimeric form of the tandem domains, they provide a specific evidence for a functional homodimer structure. Given its ideal binding mode, citrate may prove to be a potent inhibitor of the functions of FYVE domain–containing proteins.

Models for Binding of Phosphatidylinositol 3-Phosphate to the FYVE Dimer and Membrane Interaction

The bound citrate has seriously hampered our investigation of the binding of PI(3)P analogs to tandem domain crystals. Nonetheless, the mode of binding of citrate to the FYVE dimer provides an excellent paradigm for modeling a bound PI(3)P headgroup (Figure 5C). The citrate's C1 and C5 carboxylate oxygens (separated by ~7 Å) are homologous to the 1- and 3-phosphates, respectively, of PI(3)P. The orientation of the modeled PI(3)P head group is closely related to that of citrate; the 1- and 3-phosphates occupy the opening and the bottom, respectively, of the pocket. The modeling incorporates all four key features of citrate binding described above. A large portion of the PI(3)P is buried. The mode of PI(3)P binding places the 3-phosphate close to His-179 and the 1-phosphate close to His-178 and Arg-208. The sidechain of Arg-176 is juxtaposed between the 1- and 3-phosphates. Arg-181 and its symmetry-related counterpart may be involved in interacting with the inositol hydroxyl groups. Thus, the phosphate and hydroxyl groups of PI(3)P are assumed to be extensively involved in charge-coupling and hydrogen-bonding interactions with the conserved basic residues.

As in the bound citrate (Figure 5B), a protonated oxygen of the 3-phosphate (normal pK_a of 7.2) donates a hydrogen bond to the neutral His-179 sidechain. This hydrogen bond, combined with a salt link with Arg-176, fully satisfies the requirement of the 3-phosphate for

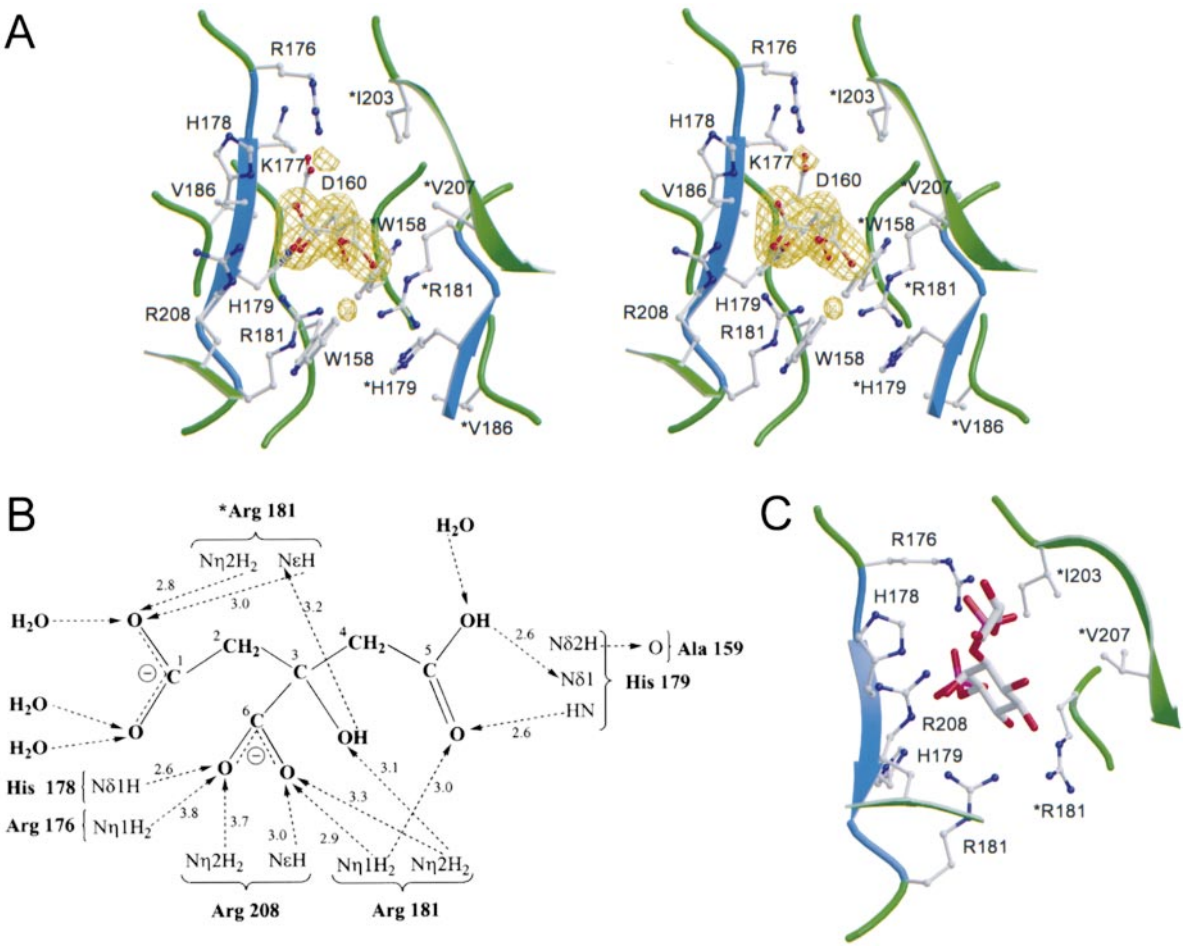

Figure 5. Multianion-Binding Site

(A) Stereo view of one of the two sites with the 2 Å resolution citrate omit (F_o-F_c), α_{calc} electron density map at $+3\sigma$. Residues from the symmetry-related FYVE domain are distinguished by asterisks.

(B) Schematic diagram of the interactions with the citrate, involving hydrogen bonds ($\leq$3.2 Å) and/or salt links ($<$4 Å), along with their observed distances in angstroms.

(C) A model of the binding of PI(3)P headgroup with a glycerol group linked to the 1-phosphate oriented toward the reader. The PI(3)P was modeled in the binding site with no steric clashes and then energy minimized using CNS (Brünger et al., 1998). Only residues within close proximity to the model are included. The 3-phosphate group, oriented away from the reader, is within hydrogen-bonding distance to His-179. The 1-phosphate moiety is close to His-178 and Arg-208. Arg-176 is within salt-linking distance to both 1- and 3 phosphates. The 2- and 3-hydroxyl groups are near Arg-181, and the 4-OH is close to Arg-181 of the symmetry-related FYVE.

ligand specificity. Furthermore, some of the nonpolar CH groups protruding from the inositol ring interface with the hydrophobic sidechains from the symmetry-related molecule identified in citrate binding (Figures 5A and 5C). The residues of the FYVE domain of EEA1 equivalent to these hydrophobic residues of Hrs, as well as the polar residues in the binding site (Figures 5A, 5B, and 5C), have been shown by NMR analysis to undergo chemical shifts upon binding of PI(3)P analogs (Kutateladze et al., 1999). Several of these shifts would not be expected if the FYVE binds PI(3)P as a monomer. The model of the Hrs FYVE-PI(3)P complex is consistent with the reasonably tight affinity (μM K_d) determined for the complex of PI(3)P analogs with the EEA1 FYVE domain (Kutateladze et al., 1999).

The model of PI(3)P binding to Hrs differs considerably from that previously proposed for the Vps27p FYVE domain (Misra and Hurley, 1999). The PI(3)P binding to a small pocket of conserved basic residues was modeled on the basis of a monomeric Vps27p FYVE structure. The modeling further relied on the observation that the pocket is occupied by two carboxylate sidechains of Asp and Glu residues from a lattice-related molecule. The locations of the Asp and Glu carboxylates, separated by about 9 Å, were assumed to be the sites for binding of the 3- and 1-phosphate groups, respectively, of the PI(3)P headgroup. The 3-phosphate lies in an approximately similar location as that of the model in Hrs FYVE dimer. However, the locations of the 1-phosphate group in the two models are completely different. As a result, the orientations of the PI(3)P headgroup with respect to the binding site differ greatly between the two models. The model with Vps27p (Misra and Hurley, 1999) places the phosphatidylinositol in an area of the monomer which, in the Hrs FYVE domain, is heavily engaged in dimer formation. The PI(3)P modeled in the

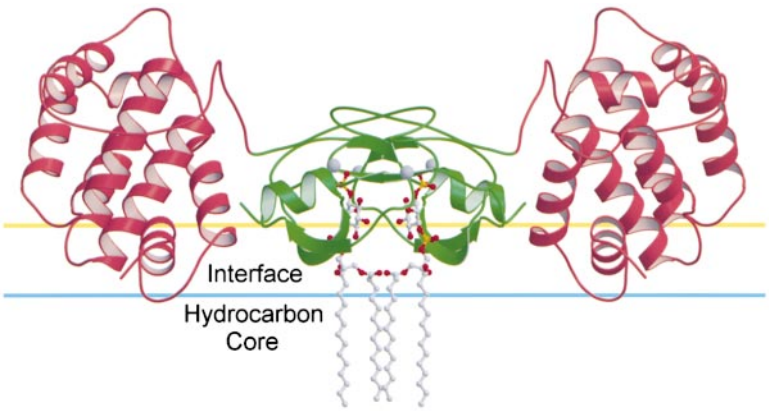

Figure 6. Model of the Interaction of the VHS and FYVE Tandem Domains with the Membrane

The flat "front" surface of the tandem domains shown in Figures 1B and 4A interfaces with the membrane. The region of the VHS domain protruding into the membrane interface contains predominantly basic residues (Arg 3, Lys-8, and Arg-18) and hydrophobic residues (Phe-2, Leu-17, and Leu-19) that could interact nonspecifically with the bilayer.

Vps27p lies sideways or parallel with respect to the β1 strand with its 1-phosphate group directed toward the apical end of the FYVE domain and engaged in an interaction with Lys-189 (the equivalent of Lys-177 of Hrs). In contrast, in our model with the Hrs homodimer, the PI(3)P is normal to the β1 strand, its 1-phosphate protruding from the opening of the pocket and far from Lys-177 (Figure 5C). Moreover, of the four key features of ligand recognition and binding to the Hrs dimer described above, only some of the electrostatic interactions may have semblance with the proposed model of PI(3)P binding to the Vps27p FYVE monomer. The monomeric binding mode, with the ligand also significantly exposed to the bulk solvent, may not be sufficient for high ligand specificity and affinity.

The difference between the two proposed PI(3)P-binding modes leads to two completely different models for membrane-targeting of the FYVE domain. In our model shown in Figure 6, the extended tandem domain dimeric structure lies in a horizontal direction with respect to the membrane surface. In addition to the association between FYVE and the phosphoinositol 3-phosphate headgroup of the membranes (Figures 5C and 6), the model would place the VHS domain in a position to interact with membranes (Figure 6), a feature consistent with the demonstration that the VHS domain interacts with the membrane (discussed above). In contrast, in the model based on the "sideways" binding of the PI(3)P proposed by Misra and Hurley (1999), the FYVE monomer lies in a vertical orientation with respect to the membrane with the tip of the apical end inserted in the membrane's interface. This orientation would place the VHS domain of Vps27p, assuming similar pyramidal arrangement with the FYVE domain as seen in the Hrs tandem domain structure, very far from the membrane surface. Finally, in contrast with the Vps27p model, the finding that the apical end of the Hrs FYVE domain is buried and extensively involved in polar and nonpolar interactions with the symmetry-related VHS domain (discussed above; Figure 1B) would completely preclude the interaction of this end with the membrane's interface.

Since the citrate or the modeled PI(3)P interacts predominantly with the basic residues of the conserved motif, ligand binding solely to one FYVE domain is not precluded. However, binding to the monomer would, as in the case also of the model with the Vps27p FYVE, lead to a more solvent exposed ligand [e.g., ~50% exposed accessible surface area of citrate or the modeled PI(3)P)] and the elimination of the hydrophobic interactions described above, resulting in weaker ligand affinities. Therefore, the functional form of the FYVE domain favors a homodimer.

Conclusion

In conclusion, the structure reported here reveals the unique superhelical conformation of the VHS domain and its relationship with the FYVE domain. It further shows the formation of a homodimer mainly through the antiparallel association of FYVE domains. The VHS domain's presence in proteins implicated in membrane trafficking, superhelical folding character, and involvement in interdomain and dimeric interactions strongly suggest that the VHS domain functions as a multipurpose docking adapter. Furthermore, the finding of the dimeric form of the FYVE domain and its complex with citrate provide an excellent paradigm for PI(3)P recognition. Based on these results, we have proposed a model for PI(3)P binding and membrane interaction of the tandem domains. Finally, the structure of the tandem domains reported here serves as a framework for further studies of Hrs and other related proteins, especially the distinct role of each domain in membrane trafficking and signal transduction events.

Experimental Procedures

Expression, Purification, and Crystallization

The DNA sequences corresponding to the tandem domains (residues 1–219) of *Drosophila* Hrs were amplified by PCR and cloned into the pTYB1 expression vector of the IMPACT T7 System (New England BioLabs) as the N-terminal segment fused to the intein and chitin-binding domain unit. To facilitate protein splicing, a glycine residue was introduced between the Hrs protein and the intein. Proteins were expressed in *Escherichia coli* ER2566 cells at room temperature, purified to near homogeneity according to the procedure provided with the IMPACT T7 System, and dialyzed against 50 mM NaCl and 100 mM Tris (pH 8.0), at 4°C. To remove minor impurities, the protein (5 mg/ml) was further purified on an HQ column, and the stock protein solution was concentrated to 10 mg/ml in 1 mM DTT and 50 mM citrate (pH 5.5). The protein was crystallized at 4°C using the vapor diffusion method with the drop consisting of a 1:1 mixture of the stock protein solution and the reservoir solution of 15% PEG 10000, 5 mM DTT, and 100 mM HEPES (pH 7.4). Prior to data collection, the crystal was flash-frozen in liquid nitrogen with 25% glycerol in the crystallization solution.

Structure Determination

The structure was determined by multiwavelength anomalous dispersion (MAD). A 3-wavelength data set was collected from a crystal of selenomethionine-substituted protein on beamline X4A at NSLS of the Brookhaven National Laboratory and processed and merged with DENZO and SCALEPACK (Otwinowski and Minor, 1997), respectively. The positions of four of the six SeMet sites and 2 Zn^{2+} were determined, heavy atom parameters refined, and MAD phases calculated at 2.4 Å resolution using the suite of programs in SOLVE (http://www.hwi.buffalo.edu/SnB). The calculated electron density map, which was solvent flattened in DM (Cowton, 1994), was used to build an initial model of 180 of the total 220 residues by means of O (Jones et al., 1991). The model was refined in CNS (Brünger et al., 1998) interspersed with model building and fitting of water molecules using CHAIN (Sack and Quiocho, 1997). Although the density of the bound citrate was well defined in initial maps, its model was fitted only in the final rounds of refinement. The final model was refined against the 2 Å resolution data (92.4% complete with 2σ cutoff) from the higher-energy remote λ_3 wavelength (Table 1).

Acknowledgments

We thank W. Meador and G. Hu for technical and software assistance; C. Ogata and R. Abramowitz for assistance with data collection at the Brookhaven National Laboratory facility; and T. Terwilliger for SOLVE. H. B. and F. A. Q. are Investigators in the Howard Hughes Medical Institute.

Received December 1, 1999; revised January 7, 2000.

References

Altschul, S.F., Madden, T.L., Schaffer, A.A., Zhang, J., Zhang, Z., Miller, W., and Lipman, D.J. (1997). Gapped BLAST and PSI-BLAST: a new generation of protein database search programs. Nucleic Acids Res. *25*, 3389–3402.

Asao, H., Sasaki, Y., Arita, T., Tanaka, N., Endo, K., Kasai, H., Takeshita, T., Endo, Y., Fujita, T., and Sugamura, K. (1997). Hrs is associated with STAM, a signal-transducing adaptor molecule. Its suppressive effect on cytokine-induced cell growth. J. Biol. Chem. *272*, 32785–32791.

Bean, A.J., Seifert, R., Chen, Y.A., Sacks, R., and Scheller, R.H. (1997). Hrs-2 is an ATPase implicated in calcium-regulated secretion. Nature *385*, 826–829.

Brünger, A.T., Adams, P.D., Clore, G.M., DeLano, W.L., Gros, P., Grosse-Kunstleve, R.W., Jiang, J.S., Kuszewski, J., Nilges, M., Pannu, N.S., et al. (1998). Crystallography and NMR system: a new software suite for macromolecular structure determination. Acta Crystallogr. D *54*, 905–921.

Burd, C.G., and Emr, S.D. (1998). Phosphatidylinositol(3)-phosphate signaling mediated by specific binding to RING FYVE domains. Mol. Cell *2*, 157–162.

Carbone, R., Fre, S., Iannolo, G., Belleudi, F., Mancini, P., Pelicci, P.G., Torrisi, M.R., and Di Fiore, P.P. (1997). eps15 and eps15R are essential components of the endocytic pathway. Cancer Res. *57*, 5498–5504.

Christoforidis, S., McBride, H.M., Burgoyne, R.D., and Zerial, M. (1999). The Rab5 effector EEA1 is a core component of endosome docking. Nature *397*, 621–625.

Cowton, K. (1994). "dm": an automated procedure for phase improvements by density modifications. Joint CCP4 and ESF-EACBM Newsletter. Protein Cryst. *31*, 34–38.

Das, A.K., Cohen, P.T.W., and Barford, D. (1998). The structure of the tetratricopeptide repeats of protein phosphatase 5: implications for TPR-mediated protein-protein interactions. EMBO J. *17*, 1192–1199.

Esnouf, R.M. (1997). An extensively modified version of MolScript that includes greatly enhanced coloring capabilities. J. Mol. Graph. Model. *15*, 132–134.

Gaullier, J.M., Simonsen, A., D'Arrigo, A., Bremnes, B., Stenmark, H., and Aasland, R. (1998). FYVE fingers bind PtdIns(3)P. Nature *394*, 432–433.

Groves, M.R., Hanlon, N., Turowski, P., Hemmings, B.A., and Barford, D. (1999). The structure of the protein phosphatase 2A PR65/A subunit reveals the conformation of its 15 tandemly repeated HEAT motifs. Cell *96*, 99–110.

Holm, L., and Sander, C. (1995). Dali: a network tool for protein structure comparison. Trends Biochem. Sci. *20*, 478–480.

Huber, A.H., Nelson, W.J., and Weis, W.I. (1997). Three-dimensional structure of the armadillo repeat region of b-catenin. Cell *90*, 871–882.

Jones, T.A., Zou, J.Y., Cowan, S.W., and Kjeldgaard, M. (1991). Improved methods for building protein models in electron density maps and the location of errors in these models. Acta Crystallogr. A *47*, 110–119.

Klein, D.E., Lee, A., Frank, D.W., Marks, M.S., and Lemmon, M.A. (1998). The pleckstrin homology domains of dynamin isoforms require oligomerization for high affinity phosphoinositide binding. J. Biol. Chem. *42*, 27725–27733.

Komada, M., and Kitamura, N. (1995). Growth factor-induced tyrosine phosphorylation of Hrs, a novel 115-kilodalton protein with a structurally conserved putative zinc finger domain. Mol. Cell Biol. *15*, 6213–6221.

Komada, M., and Soriano, P. (1999). Hrs, a FYVE finger protein localized to early endosomes, is implicated in vesicular traffic and required for ventral folding morphogenesis. Genes Dev. *13*, 1475–1485.

Komada, M., Masaki, R., Yamamoto, A., and Kitamura, N. (1997). Hrs, a tyrosine kinase substrate with a conserved double zinc finger domain, is localized to the cytoplasmic surface of early endosomes. J. Biol. Chem. *272*, 20538–20544.

Kraulis, P.J. (1991). MOLSCRIPT: a program to produce both detailed and schematic plots of protein structures. J. Appl. Cryst. *24*, 946–950.

Kutateladze, T.G., Ogburn, K.D., Watson, W.T., de Beer, T., Emr, S.D., Burd, C.G., and Overduin, M. (1999). Phosphatidylinositol 3-phosphate recognition by the FYVE domain. Mol. Cell *3*, 805–811.

Lohi, O., and Lehto, V.P. (1998). VHS domain marks a group of proteins involved in endocytosis and vesicular trafficking. FEBS Lett. *440*, 255–257.

Lohi, O., Poussu, A., Merilainen, J., Kellokumpu, S., Wasenius, V.M., and Lehto, V.P. (1998). EAST, an epidermal growth factor receptor- and eps15-associated protein with Src homology 3 and tyrosine-based activation motif domains. J. Biol. Chem. *273*, 21408–21415.

Merritt, E.A., and Bacon, D.J. (1997). Raster3D version 2.0: a program for photorealistic molecular graphics. Methods Enzymol. *277*, 505–524.

Misra, S., and Hurley, J.H. (1999). Crystal structure of a phosphatidylinositol 3-phosphate-specific membrane-targeting motif, the FYVE domain of Vps27p. Cell *97*, 657–666.

Nicholls, A., Bharadwaj, R., and Honig, B. (1993). GRASP: graphical representation and analysis of surface properties. Biophys. J. *64*, 166–170.

Otwinowski, Z., and Minor, W. (1997). Processing of X-ray diffraction data collected in oscillation mode. Methods Enzymol. *276*, 307–326.

Patki, V., Lawe, D.C., Corvera, S., Virbasius, J.V., and Chawla, A. (1998). A functional PtdIns(3)P-binding motif. Nature *394*, 433–434.

Piper, R.C., Cooper, A.A., Yang, H., and Stevens, T.H. (1995). VPS27 controls vacuolar and endocytic traffic through a prevacuolar compartment in Saccharomyces cerevisiae. J. Cell. Biol. *131*, 603–617.

Raag, R., Appelt, K., Xuong, N.H., and Banaszak, L. (1988). Structure of the lamprey yolk lipid-protein complex lipovitellin- phosvitin at 2.8 Å resolution. J. Mol. Biol. *200*, 553–569.

Sack, J.S., and Quiocho, F.A. (1997). CHAIN-A crystallographic modeling program. Methods Enzymol. *277*, 158–173.

Simonsen, A., Lippe, R., Christoforidis, S., Gaullier, J.M., Brech, A., Callaghan, J., Toh, B.H., Murphy, C., Zerial, M., and Stenmark, H. (1998). EEA1 links PI(3)K function to Rab5 regulation of endosome fusion. Nature *394*, 494–498.

Stenmark, H., Aasland, R., Toh, B.H., and D'Arrigo, A. (1996). Endosomal localization of the autoantigen EEA1 is mediated by a zinc-binding FYVE finger. J. Biol. Chem. *271*, 24048–24054.

Strickland, C.L., Windsor, W.T., Syto, R., Wang, L., Bond, R., Wu, Z., Schwartz, J., Le, H.V., Beese, L.S., and Weber, P.C. (1998). Crystal structure of farnesyl protein transferase complexed with a CaaX peptide and farnesyl diphosphate analogue. Biochemistry *37*, 16601–16611.

Takeshita, T., Arita, T., Asao, H., Tanaka, N., Higuchi, M., Kuroda, H., Kaneko, K., Munakata, H., Endo, Y., Fujita, T., et al. (1996). Cloning of a novel signal-transducing adaptor molecule containing an SH3 domain and ITAM. Biochem. Biophys. Res. Commun. *225*, 1035–1039.

Takeshita, T., Arita, T., Higuchi, M., Asao, H., Endo, K., Kuroda, H., Tanaka, N., Murata, K., Ishii, N., and Sugamura, K. (1997). STAM, signal transducing adaptor molecule, is associated with Janus kinases and involved in signaling for cell growth and c-myc induction. Immunity *6*, 449–457.

Tall, G.G., Hama, H., DeWald, D.B., and Horazdovsky, B.F. (1999). The phosphatidylinositol 3-phosphate binding protein Vac1p interacts with a Rab GTPase and a Sec1p homologue to facilitate vesicle-mediated vacuolar protein sorting. Mol. Biol. Cell *10*, 1873–1889.

Thunnissen, A.M., Dijkstra, A.J., Kalk, K.H., Rozeboom, H.J., Engel, H., Keck, W., and Dijkstra, B.W. (1994). Doughnut-shaped structure of a bacterial muramidase revealed by X-ray crystallography. Nature *367*, 750–753.

Vetter, I.R., Arndt, A., Kutay, U., Gorlich, D., and Wittinghofer, A. (1999). Structural view of the Ran-Importin β interaction at 2.3 Å resolution. Cell *97*, 635–646.

Protein Data Bank ID Code

Atomic coordinates have been deposited with the ID code 1DVP.